論文

Moisture Induced Boundary-Layer Transient Stresses in Orthotropic Shells under External Pressure

Chang-Bum Chung*

직등방성 쉘 구조물이 외압을 받을 때 흡습에 기인한 경계층 천이 응력

정 창 범*

초 록

흡습에 기인한 높은 응력들이 고전 래미네이션 이론으로는 정확하게 평가될 수 없는 경계층 영역과 가장자리로부터 몇 개의 래미나 두께들 안의 국소 영역에서 발생된다고 보고되고 있다. 이러한 높은 응력이 발생하는 경계층 영역의 거동은 복합재 성능 및 복잡한 파손모드를 조절하는데 극히 중요하다. 이 논문에서는 첫째, 두꺼운 복합재 쉘 구조물에 대한 흡습에 기인한 천이 응력과 변형률에 대한 기준해를 제공하며, 둘째로는 외압과 흡습에 기인한 응력이 동시에 작용하는 경우에 대한 응력변화를 연구한다.

ABSTRACT

The high hygroscopic stresses are reported to be confined within a localized region of several laminar thicknesses from the edge, and in the boundary-layer region they cannot be assessed accurately with classical lamination theory. The behavior of this highly stressed boundary-layer region is of great importance in controlling the complex failure modes and performance of the composite. This study includes (i) providing a benchmark solution for the moisture induced transient stress and strain fields, and (ii) investigating the stress field produced by the combined influence of the transient moisture induced stresses and the external pressure in a thick composite shell structure.

1. Introduction

Shell structures are broadly used in industries as load-carrying elements. In particular, composite shell structures have many applications in the aerospace industry, in which weight optimization should be considered. Although thin shell constructions have been used in many applications, the use of moderately thick composite shells is now being considered in the marine and automobile industries as well as for components in the aerospace industry. Moreover, composites in the form of circular cylindrical shells are considered for civil engineering, column-type applications and in space vehicles as a primary, load-carrying structure.

The understanding of the stresses induced by moisture in a composite structure is essential for the design and the comprehensive

* 삼성항공 우주연구소

study of its response during service in severe hygroscopic environments.

Browning, Husman, and Whitney[1] showed through experiments that temperature and moisture cause the strength and the mechanical property of a material to be degraded. They explained that the two sources of the degradation could be the change of the glass transition temperature and the residual stresses in the interfaces due to the moisture absorption. The two sources induce failure mode change from the fiber dominated failure to the matrix dominated one. Their experimental data indicated that the degradation occurs more severely in the direction transverse to the fibers than in the longitudinal one. Whitney and Husman[2] proposed that a flexure test provides a simple means for determining hygrothermal conditions which induce the degradation of the strength and the material properties.

DeIasi and Whiteside[3] showed experimentally that the value of the moisture diffusivity increases as temperature or relative humidity increases, and the glass transition temperature decreases as the moisture content increases. For the swelling induced by moisture absorption, Hahn et al.[4,5,6] calculated the residual stresses resulting from the difference in the swelling between fibers and matrix through micromechanics analysis. They suggested that the residual stress may lead to the creation of microcracks and further degrade the strength and mechanical properties of composites. Crossman, Mauri and Warren[7] suggested that moisture distribution alters the viscoelastic response of composites.

Harper[8] used the energy method and classical lamination theory with Kirchhoff's assumptions for displacement fields to show the change of curvature in anti-symmetric cross-ply laminates due to moisture absorption. His results showed that moisture distribution plays an important role on the deformed shapes of the laminates. Pipes, Vinson and Chou[9] used the classical lamination theory to analyze the stress field, with the resultant forces and moments caused by environmental stresses derived from the Fickian diffusion equation. Kardomateas[10,11] used a displacement approach and a series expansion technique to solve the transient thermal stress problem in composite cylinders. He modified the displacement field in the axisymmetric, time-independent conditions derived by Lekhnitskii[12], for time-dependent thermal stress problems (which are analogous to the time-dependent moisture induced stress problems).

Chung[13,14] analyzed a moisture induced transient stress problem by use of three-dimensional elasticity and Kardomateas' modified displacement field[10]. He showed the variation of moisture content and stresses with respect to time and radial distance along the thickness.

Doxee and Springer[15] analyzed hygrothermal stresses and strains in an axisymmetric composite shell according to Doxee's higher-order shell theory[16]. Farley and Herakovich[17] suggested that the gradient of moisture concentration is an important factor in altering stress distributions and especially, the steep gradient of moisture concentration observed in the boundary-layer region. Out of the boundary-layer region, the stress distribution is shown to be very similar to the one caused by uniform hygroscopic conditions. Wang and Choi[18] studied the hygroscopic stress field in the boundary-layer region of composite laminates subjected to uniformly distributed moisture change. They solved for the boundary-layer stresses by introducing a proper form of the Lekhnitskii[12] complex stress functions and using an eigenfunction expansion method and a boundary-collocation technique. The hygroscopic stress field in the boundary-layer region is inherently thre-

e-dimensional in nature and is singular. They proposed that the boundary-layer hygroscopic stresses may be primarily responsible for unanticipated failure of composite structures, frequently initiated at the edges.

In this paper, an accurate elasticity solution will be obtained for the stresses and displacemets in a composite shell loaded by an external pressure in a hygroscopic environment. It will be shown that the hygroscopic stress are confined for practical time values to a boundary-layer region near the surfaces (since the moisture diffusion process is relatively slow). Results will be presented that illustrate the steep gradients of moisture concentration in the boundary-layer region and of the stress distributions along the radial distance with respect to time and applied pressures.

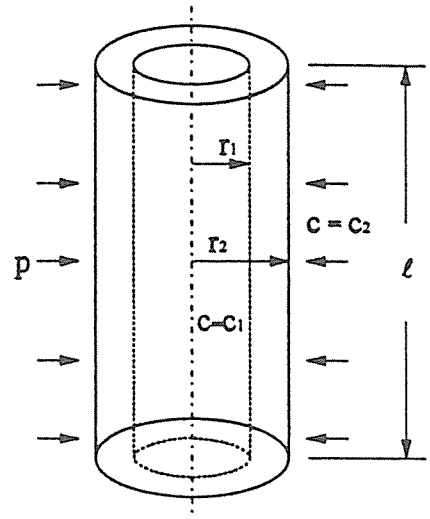

Fig. 2.1. Thick Cylindrical Shell Under Constant Boundary Concentrations of Moisture.

2. Mathematical Formulation

A problem of transient hygroscopic stresses in a hollow orthotropic circular cylinder loaded by external pressure is examined. Consider a hollow cylinder, in general under external pressure p, as shown in Fig. 2.1. The cylinder has an inner radius, r_1 and an outer radius, r_2. The radial, circumferential and axial coordinates are denoted by r, θ and z, respectively.

It is assumed that the initial concentration (at t=0) is C_0. For $t > 0$, the boundaries $r = r_1$ and $r = r_2$ are kept at constant concentrations C_1 and C_2, respectively. The reference concentration is taken as zero.

2-1. Fickian Diffusion Equation

The moisture problem is solved by the Fickian diffusion equation:

$$\frac{\partial C(r,t)}{\partial t} = D\frac{1}{r}\frac{\partial}{\partial r}(r\frac{\partial C}{\partial r}), \qquad \text{at } r_1 \le r \le r_2 \quad \cdots\cdots \text{(1a)}$$

where $C(r,t)$ is the moisture concentration and D is the moisture diffusivity of the composite in the r direction. The initial and boundary conditions are

$$C(r,t=0) = C_0, \qquad \text{at } r_1 \le r \le r_2 \quad \cdots\cdots \text{(1b)}$$

$$C(r_1,t) = C_1 \ (t>0) \text{ and } C(r_2,t) = C_2 \ (t>0) \quad \cdots\cdots \text{(1c)}$$

where C_0, C_1 and C_2 are constants.

Crank[19] gives the general solution for the distribution of the concentration of moisture $C(r,t)$ to Eq. (1) in terms of the Bessel functions of the first and second kind J_n and Y_n, as follows:

$$C(r,t) = b_1\ln(r/r_1) + b_2\ln(r_2/r) + \sum_{n=1}^{\infty}[c_n J_0(r\alpha_n) + d_n Y_0(r\alpha_n)]e^{-D\alpha_n^2 t}, \quad \cdots\cdots \text{(2a)}$$

where

$$b_1 = \frac{C_2}{\ln(r_2/r_1)}; \quad b_2 = \frac{C_1}{\ln(r_2/r_1)}, \quad \cdots\cdots \text{(2b)}$$

$$c_n = \pi C_0 \frac{J_0(r_1\alpha_n)Y_0(r_2\alpha_n)}{J_0(r_1\alpha_n)+J_0(r_2\alpha_n)} - \pi J_0(r_1\alpha_n)Y_0(r_2\alpha_n)$$
$$\frac{C_2 J_0(r_1\alpha_n) - C_1 J_0(r_2\alpha_n)}{J_0^2(r_1\alpha_n) - J_0^2(r_2\alpha_n)}, \quad \cdots\cdots (2c)$$

$$d_n = -\pi C_0 \frac{J_0(r_1\alpha_n)J_0(r_2\alpha_n)}{J_0(r_1\alpha_n)+J_0(r_2\alpha_n)} + \pi J_0(r_1\alpha_n)J_0(r_2\alpha_n)$$
$$\frac{C_2 J_0(r_1\alpha_n) - C_1 J_0(r_2\alpha_n)}{J_0^2(r_1\alpha_n) - J_0^2(r_2\alpha_n)}, \quad \cdots\cdots (2d)$$

and α_n are the positive roots of :

$$J_0(r_1\alpha_n)Y_0(r_2\alpha_n) - J_0(r_2\alpha_n)Y_0(r_1\alpha_n) = 0 \quad \cdots\cdots (2e)$$

2-2. Hygroelastic Equations

The hygroscopic stress-strain relations for the orthotropic body are

$$\begin{pmatrix} \sigma_{rr} \\ \sigma_{\theta\theta} \\ \sigma_{zz} \\ \tau_{\theta z} \\ \tau_{zr} \\ \tau_{r\theta} \end{pmatrix} = \begin{pmatrix} C_{11} & C_{12} & C_{13} & 0 & 0 & 0 \\ C_{12} & C_{22} & C_{23} & 0 & 0 & 0 \\ C_{13} & C_{23} & C_{33} & 0 & 0 & 0 \\ 0 & 0 & 0 & C_{44} & 0 & 0 \\ 0 & 0 & 0 & 0 & C_{55} & 0 \\ 0 & 0 & 0 & 0 & 0 & C_{66} \end{pmatrix} \begin{pmatrix} \varepsilon_{rr} - \beta_r \Delta C \\ \varepsilon_{\theta\theta} - \beta_\theta \Delta C \\ \varepsilon_{zz} - \beta_z \Delta C \\ \gamma_{\theta z} \\ \gamma_{zr} \\ \gamma_{r\theta} \end{pmatrix} \quad \cdots\cdots (3)$$

where c_{ij} are the elastic constants and β_i the swelling coefficients (1, 2 and 3 represent r, θ and z, respectively). The geometry (Fig. 2.1) is axisymmetric. Since the moisture concentration is assumed to depend only on the r direction, the stresses are independent of θ and z and the hoop displacement is zero. In addition to the constitutive equation (3), the equilibrium equations have to be satisfied; since $\tau_{r\theta} = \tau_{rz} = \tau_{\theta z} = 0$, only one equilibrium equation remains:

$$\frac{\partial \sigma_{rr}}{\partial r} + \frac{\sigma_{rr} - \sigma_{\theta\theta}}{r} = 0, \quad \cdots\cdots (4)$$

2-3. Displacement Approach

In this work the displacement field derived by Lekhnitskii[12] for time-independent problems and modified by Kardomateas[10] for time-dependent thermal stress problems (which are analogous to the time-dependent moisture-induced stress problems) is used[13, 14]:

$$u_r = U(r,t) + z(w_y\cos\theta - w_x\sin\theta) + u_0\cos\theta + v_0\sin\theta,$$
$$u_\theta = -z(w_y\sin\theta + w_x\cos\theta) + w_z r - u_0\sin\theta + v_0\cos\theta,$$
$$u_z = zf(t) - r(w_y\cos\theta - w_x\sin\theta) + w_0, \quad \cdots\cdots (5)$$

where the function $U(r,t)$ represents the radial displacement accompanied by deformation. The constants u_0, v_0 and w_0 denote the rigid body translation along the x, y and z directions in the Cartesian coordinate system, respectively, and w_x, w_y and w_z denote the rigid body rotation in the x,y and z directions (these may also be functions of time, but since they do not appear in the strain expressions, such a dependence would not affect the expressions that follow in this section).

The parameter $f(t)$ is obtained from boundary conditions, as discussed later. The strains are expressed in terms of the displacements as follows:

$$\varepsilon_{rr} = \frac{\partial U(r,t)}{\partial r}, \quad \varepsilon_{\theta\theta} = \frac{U(r,t)}{r}, \quad \varepsilon_{zz} = f(t)$$
$$\gamma_{\theta z} = \gamma_{zr} = \gamma_{r\theta} = 0 \quad \cdots\cdots (6)$$

Substituting Eqs. (6) and (3) into the equilibrium Eq. (4) gives the following differential equation for $U(r,t)$:

$$c_{11}\left[\frac{\partial^2 U(r,t)}{\partial r^2} + \frac{1}{r}\frac{\partial U(r,t)}{\partial r}\right] - \frac{c_{22}}{r^2}U(r,t) =$$
$$q_1\frac{\partial C(r,t)}{\partial r} + q_2\frac{C(r,t)}{r} + (c_{23} - c_{13})\frac{f(t)}{r}, \quad \cdots (7a)$$

where

$$q_1 = c_{11}\beta_r + c_{12}\beta_\theta + c_{13}\beta_z, \quad \cdots\cdots (7b)$$

$$q_2=(c_{11}-c_{12})\beta_r+(c_{12}-c_{22})\beta_\theta+(c_{13}-c_{23})\beta_z\ . \quad \cdots\cdots (7c)$$

Now set $f(t)$ in the form

$$f(t)=f_0+\sum_{n=1}^{\infty}f_n e^{-D\alpha_n^2 t}\ . \quad \cdots\cdots (8)$$

Moreover, to solve Eq. (7), set

$$U(r,t)=U_0(r)+\sum_{n=1}^{\infty}R_n(r)e^{-D\alpha_n^2 t}\ . \quad \cdots\cdots (9)$$

Substituting Eqs. (2), (8) and (9) into Eq. (7a) yields the following equations to be satisfied for U_0, and R_n for n=1,2,$\cdots\infty$:

$$c_{11}U_0''(r)+\frac{c_{11}}{r}U_0'(r)-\frac{c_{22}}{r^2}U_0(r)=\frac{c_{23}-c_{13}}{r}f_0+ q_1\frac{b_1-b_2}{r}+q_2b_1\frac{\ln(r/r_1)}{r}+q_2b_2\frac{\ln(r_2/r)}{r}\ , \quad \cdots (10a)$$

$$c_{11}R_n''(r)+\frac{c_{11}}{r}R_n'(r)-\frac{c_{22}}{r^2}R_n(r)=\frac{c_{23}-c_{13}}{r}f_n+ c_n\left[q_2\frac{J_0(r\alpha_n)}{r}-q_1\alpha_n J_1(r\alpha_n)\right]+d_n\left[q_2\frac{Y_0(r\alpha_n)}{r}-q_1\alpha_n Y_1(r\alpha_n)\right] \qquad n=1,\cdots\infty\ . \quad \cdots\cdots (10b)$$

For each of the previous equations, the solution is the sum of a homogeneous solution and a particular one. The solution of the homogeneous equation is in the form $G_1(t)r^{\lambda_1}+G_2(t)r^{\lambda_2}$

$$\lambda_{1,2}=\pm\sqrt{c_{22}/c_{11}}\ . \quad \cdots\cdots (10c)$$

In a similar fashion to the parameter $f(t)$, set $G_i(t)$ in the form: $G_i(t)=G_{i0}+\sum G_{in}e^{-D\alpha_n^2 t}$, i=1,2.

Since the constants f_n and G_{ij} are yet unknown, we shall indicate the places where they enter in the expressions that follow (these constants are found later from the boundary conditions). For $c_{11}\neq c_{22}$ the solution of (10a) for $U_0(r)$ is

$$U_0(r)=G_{10}r^{\lambda_1}+G_{20}r^{\lambda_2}+\frac{c_{23}-c_{13}}{c_{11}-c_{22}}f_0 r+U_0^*(r)\ , \quad \cdots\cdots (11a)$$

where

$$U_0^*(r)=\frac{q_2b_1}{c_{11}-c_{22}}r\ln(r/r_1)+\frac{q_2b_2}{c_{11}-c_{22}}r\ln(r_2/r)+ +\frac{[q_1(c_{11}-c_{22})-2q_2c_{11}]}{(c_{11}-c_{22})^2}(b_1-b_2)r\ . \quad \cdots\cdots (11b)$$

For $c_{11}=c_{22}$ the corresponding solution of (10a) is

$$U_0(r)=G_{10}r+\frac{G_{20}}{r}+\frac{c_{23}-c_{13}}{2c_{11}}f_0 r\ln(r/r_1)+U_0^*(r)\ , \quad \cdots\cdots (12a)$$

where

$$U_0^*(r)=\frac{q_2b_1}{4c_{11}}r\ln^2(r/r_1)-\frac{q_2b_2}{4c_{11}}r\ln^2(r_2/r)+ \frac{(2q_1-q_2)(b_1-b_2)}{4c_{11}}r\ln(r/r_1)\ . \quad \cdots\cdots (12b)$$

To solve (10b) we use the series expansions of the Bessel functions to obtain a series expansion of the right-hand side, as given in Appendix A. In the following, γ stands for the Euler's constant ($\simeq$ 0.577215...).

For $c_{11}\neq c_{22}$, the resulting equation (A5) in Appendix A leads to the solution of (10b) for R_n, $n=1,\cdots\infty$, as follows:

$$R_n(r)=G_{1n}r^{\lambda_1}+G_{2n}r^{\lambda_2}+\frac{c_{23}-c_{13}}{c_{11}-c_{22}}f_n r+R_n^*(r)\ , \quad \cdots\cdots (13a)$$

$$R_n^*(r)=B_{0n}r+\frac{2q_2d_n}{\pi(c_{11}-c_{22})}r\ln(r\alpha_n/2)+\sum_{k=0}^{\infty} B_{1nk}r^{2k+3}\ln(r\alpha_n/2)+B_{2nk}r^{2k+3}\ , \quad \cdots\cdots (13b)$$

where

$$B_{0n}=\frac{c_n q_2+d_n(2/\pi)(q_1+\gamma q_2)}{c_{11}-c_{22}}-\frac{4c_{11}q_2d_n}{\pi(c_{11}-c_{22})^2}. \quad \cdots\cdots (13c)$$

The coefficients in the sum over k are given in terms of

$$f_{kn}=\left[c_n-\frac{2d_n}{\pi}\left(1+\frac{1}{2}+\cdots+\frac{1}{k+1}-\gamma\right)\right][q_2+2q_1(k+1)]+\frac{2d_nq_1}{\pi}, \quad \cdots\cdots (13d)$$

as follows:

$$B_{1nk}=\frac{2d_n(-1)^{k+1}\alpha_n^{2k+2}[q_2+2q_1(k+1)]}{\pi\,2^{2k+2}[(k+1)!]^2[c_{11}(2k+3)^2-c_{22}]}, \quad \cdots\cdots (14a)$$

$$B_{2nk}[c_{11}(2k+3)^2-c_{22}]=\frac{(-1)^{k+1}\alpha_n^{2k+2}}{2^{2k+2}[(k+1)!]^2}f_{kn}-B_{1nk}\,2c_{11}(2k+3). \quad \cdots\cdots (14b)$$

In the (unlikely) event that for a certain k, $c_{11}(2k+3)^2=c_{22}$, the term in the sum for this k is replaced by (A13) with (A14) and (A15) in Appendix A.

For $c_{11}=c_{22}$ the solution of (10b) for R_n is

$$R_n(r)=G_{1n}r+\frac{G_{2n}}{r}+\frac{c_{23}-c_{13}}{2c_{11}}f_n r\ln(r/r_1)+R_n^*(r), \quad \cdots\cdots (15a)$$

$$R_n^*(r)=B_{0n}r\ln(r\,\alpha_n/2)+\frac{d_nq_2}{2\pi c_{11}}r\ln^2(r\,\alpha_n/2)+\sum_{k=0}^{\infty}B_{1nk}r^{2k+3}\ln(r\,\alpha_n/2)+B_{2nk}r^{2k+3}, \quad \cdots\cdots (15b)$$

where

$$B_{0n}=\frac{\pi c_n q_2+d_n(2q_1+2\gamma q_2-q_2)}{2\pi c_{11}}. \quad \cdots\cdots (15c)$$

The series expansion for the Bessel functions cannot be used for large arguments; hence, the requirement of including an increasing number of terms and therefore large arguments, necessitates finding a particular solution for the "large arguments" domain. This is achieved by using the Hankel asymptotic expansions of the Bessel functions of the first and second kind (see (A6) through (A12) in Appendix A). Employing the substitution

$$\rho=r\,\alpha_n\ ;\ R_n^{**}(\rho)=R_n^*(r), \quad \cdots\cdots (16)$$

gives the following equation for $R_n^{**}(\rho)$

$$c_{11}\alpha_n^2\left(R_n^{**\prime\prime}(\rho)+\frac{R_n^{**\prime}(\rho)}{\rho}\right)-c_{22}\alpha_n^2\frac{R_n^{**}(\rho)}{\rho^2}=\sum_{k=0}^{\infty}\frac{(-1)^k\alpha_n\psi_1(k)}{(2k)!(8\rho)^{2k}\rho\sqrt{\pi\rho}}\times\{(c_n+d_n)(q_2\sin\rho-a_{1,k}\rho\cos\rho+a_{2,k}\rho^2\sin\rho)+(c_n-d_n)(q_2\cos\rho+a_{1,k}\rho\sin\rho+a_{2,k}\rho^2\cos\rho)\}, \quad \cdots\cdots (17)$$

where

$$a_{1,k}=q_1\frac{4k+1}{4k-1}-q_2\frac{16k}{(4k-1)^2}\ ;\ a_{2,k}=\frac{16kq_1}{(4k-1)(4k-3)}, \quad \cdots\cdots (18)$$

and $\psi_1(k)$ is defined by (A8) in Appendix A.

The solution of the above equation for the function $R_n^{**}(\rho)$ is found to be

$$R_n^{**}(\rho)=\sum_{k=0}^{\infty}p_{k,1}^n\rho^{-2k-1/2}\cos\rho+s_{k,1}^n\rho^{-2k-1/2}\sin\rho+p_{k,2}^n\rho^{-2k-3/2}\cos\rho+s_{k,2}^n\rho^{-2k-3/2}\sin\rho. \quad \cdots\cdots (19a)$$

The coefficients $p_{k,1}^n, s_{k,1}^n, p_{k,2}^n, s_{k,2}^n$ are determined by considering the terms in the sum that contribute to the terms $\rho^{-2k-1/2}\cos\rho$, $\rho^{-2k-1/2}\sin\rho$, $\rho^{-2k-3/2}\cos\rho$, $\rho^{-2k-3/2}\sin\rho$ in the right hand side of (17). Define

$$D_k=\frac{(-1)^k\psi_1(k)}{(2k)!8^{2k}\alpha_n\sqrt{\pi}}. \quad \cdots\cdots (19b)$$

We obtain the following recursive formulas for $p^n_{k,1}$, $s^n_{k,1}$,

$$p^n_{k,1}c_{11} = p^n_{k-1,1}[c_{11}(2k-3/2)^2 - c_{22}] - s^n_{k-1,2}c_{11}(4k-2) + D_k a_{1,k}(c_n + d_n), \quad \cdots\cdots (20a)$$

$$s^n_{k,1}c_{11} = s^n_{k-1,1}[c_{11}(2k-3/2)^2 - c_{22}] + p^n_{k-1,2}c_{11}(4k-2) - D_k a_{1,k}(c_n - d_n), \quad \cdots\cdots (20b)$$

and for $p^n_{k,2}$, $s^n_{k,2}$,

$$p^n_{k,2}c_{11} = p^n_{k-1,2}[c_{11}(2k-1/2)^2 - c_{22}] - s^n_{k,1}c_{11}4k - -(D_k q_2 + D_{k+1}a_{2,k+1})(c_n - d_n), \quad \cdots\cdots (20c)$$

$$s^n_{k,2}c_{11} = s^n_{k-1,2}[c_{11}(2k-1/2)^2 - c_{22}] + p^n_{k,1}c_{11}4k - -(D_k q_2 + D_{k+1}a_{2,k+1})(c_n + d_n). \quad \cdots\cdots (20d)$$

The process starts from $k=1$ and the starting values for $k=0$ are from (17) and (18) as follows:

$$p^n_{0,1} = -\frac{q_1(c_n + d_n)}{c_{11}\alpha_n\sqrt{\pi}}; \quad s^n_{0,1} = \frac{q_1(c_n - d_n)}{c_{11}\alpha_n\sqrt{\pi}}, \quad \cdots (21a)$$

$$p^n_{0,2} = (-8q_2 + 3q_1)\frac{(c_n - d_n)}{8c_{11}\alpha_n\sqrt{\pi}};$$

$$s^n_{0,2} = (-8q_2 + 3q_1)\frac{(c_n + d_n)}{8c_{11}\alpha_n\sqrt{\pi}}. \quad \cdots\cdots (21b)$$

An important issue regarding this analysis will be dicussed now. The solution (19) is a particular solution of equation (17), derived by considering the Hankel asymptotic expansions of the Bessel functions for values of the argument $\rho = r\alpha_n \geq \rho_{tr} = 18.0$ (see Appendix A), whereas the solution (13b), which will be denoted by $R^*_{nS}(r)$, had been derived based on a series expansion for the Bessel functions, for values of the argument $\rho \leq \rho_{tr}$. Since for a given root α_n the argument ρ ranges from $r_1\alpha_n$ to $r_2\alpha_n$, there may be a transition point from one solution to the other for $R^*_n(r)$ in the expression (15a). Both solutions are particular ones and may be different. Therefore, at that transition point a homogeneous solution term should be added to (19) so that

$$R^{**}_{nL}(\rho) = h_{1n}\rho^{\lambda_1} + h_{2n}\rho^{\lambda_2} + R^{**}_n(\rho); \quad R^*_n(r) = R^{**}_{nL}(\rho), \quad \cdots\cdots (22a)$$

where h_{1n} and h_{2n} are determined from the condition of equal value and slope at the transition point

$$R^{**}_{nL}(\rho_{tr}) = R^*_{nS}(\rho_{tr}/\alpha_n); \quad R^{**}_{nL}{}'(\rho_{tr})\alpha_n = R^*_{nS}{}'(\rho_{tr}/\alpha_n). \quad \cdots\cdots (22b)$$

Thus, the expression for $U(r,t)$ satisfying the equlibrium equations is obtained with the unknown coefficients G_{10} , G_{20} , f_0 ; G_{1n} , G_{2n} and f_n for $n=1,2\cdots$. These coefficients are determined from the following boundary conditions:

$$\sigma_{rr}(r_1,t) = 0, \ \sigma_{rr}(r_2,t) = -p \ ; \ \tau_{r\theta}(r_i,t) = \tau_{rz}(r_i,t) = 0, \quad i = 1,2. \quad \cdots\cdots (23)$$

where p is the external pressure. Only those for the stress σ_{rr} are not identically satisfied. The stress σ_{rr} on the boundaries is written in terms of the displacement field:

$$\sigma_{rr}(r_i,t) = c_{11}U_{,r}(r_i,t) + c_{12}\frac{U(r_i,t)}{r} + c_{13}f(t) - q_1 C(r_i,t), \ i=1,2, \quad \cdots\cdots (24)$$

Substituting Eqs. (2), (8), (9) into (24) for $U_0(r)$ gives the following two linear equations for G_{10},G_{20} and f_0 :

$$(c_{11}\lambda_1 + c_{12})r_i^{\lambda_1 - 1}G_{10} + (c_{11}\lambda_2 + c_{12})r_i^{\lambda_2 - 1}G_{20} + A_0 f_0 = = -c_{11}U^*_0{}'(r_i) - c_{12}\frac{U^*_0(r_i)}{r_i} + q_1[b_1\ln(r_i/r_1) + b_2 \ln(r_2/r_i)] + p_i \quad i=1,2, \quad (25a)$$

where

$$A_0 = \frac{c_{11} + c_{12}}{c_{11} - c_{22}}(c_{23} - c_{13}) + c_{13} \qquad \text{for} \quad c_{11} \neq c_{22},$$

..... (25b)

$$= \frac{c_{23}-c_{13}}{2c_{11}}[c_{11}+(c_{11}+c_{12})\ln(r_i/r_1)]+c_{13} \text{ for } c_{11}=c_{22}$$

and $p_i = 0$, at $i=1$; $p_i = -p$ at $i=2$.

In a similar fashion, by substituting the expressions for $R_n(r)$, there correspond two linear equations for G_{1n}, G_{2n}, f_n, for $n=1,\cdots\infty$, as follows,

$$(c_{11}\lambda_1+c_{12})r_i^{\lambda_1-1}G_{1n}+(c_{11}\lambda_2+c_{12})r_i^{\lambda_2-1}G_{2n}+A_0 f_n =$$
$$= -c_{11}R_n^{*\prime}(r_i) - c_{12}\frac{R_n^*(r_i)}{r_i} + q_1[c_n J_0(r_i\alpha_n)+$$
$$d_n Y_0(r_i\alpha_n)]; \quad i=1,2. \quad \cdots\cdots (25c)$$

Now, let us consider the conditions of resultant forces and moments. Since the stresses do not depend on z, these conditions exist in any cross section. It can be proved (e.g. Lehknitskii [12], although hygroscopic effects are not included) that the conditions of zero resultant forces along the x and y axes of a Cartesian coordinate system are satisfied identically. The conditions of zero resultant moment along x and y axes (and that of zero twisting moment) are also satisfied by the symmetry of the problem. Therefore, it remains only the condition of resultant axial force, P_z, arising in a hydrostatic field:

$$\int_{r_1}^{r_2}\sigma_{zz}(r,t)\,2\pi r dr = P_z(t) = -p\pi(r_2^2-r_1^2). \quad \cdots\cdots (26)$$

This gives the last set of equations that are needed to determine the constants G_{ij}, f_i. In terms of

$$q_3 = c_{13}\beta_r + c_{23}\beta_\theta + c_{33}\beta_z, \quad \cdots\cdots (27)$$

Equation (26) gives

$$\left(\frac{c_{13}\lambda_1+c_{23}}{\lambda_1+1}\right)(r_2^{\lambda_1+1}-r_1^{\lambda_1+1})G_{10}+A_1G_{20}+A_2f_0 =$$
$$= (c_{13}-c_{23})I_0 + \frac{q_3}{2}\left[\frac{(r_2^2-r_1^2)}{2}(b_2-b_1)+(r_2^2b_1-\right.$$
$$\left. r_1^2b_2)\ln(r_2/r_1)\right] - \frac{p}{2}(r_2^2-r_1^2)+c_{13}\sum_{i=1,2}(-1)^{i+1}r_i$$
$$U_0^*(r_i), \quad \cdots\cdots (28a)$$

and for $n=1,\cdots\infty$,

$$\left(\frac{c_{13}\lambda_1+c_{23}}{\lambda_1+1}\right)(r_2^{\lambda_1+1}-r_1^{\lambda_1+1})G_{1n}+A_1G_{2n}+A_2f_n =$$
$$(c_{13}-c_{23})I_n + c_{13}\sum_{i=1,2}(-1)^{i+1}r_iR_n^*(r_i)+(q_3/\alpha_n)(-1)^i$$
$$[c_n r_i J_1(r_i\alpha_n)+d_n r_i Y_1(r_i\alpha_n)], \quad \cdots\cdots (28b)$$

where I_0 and I_n are given by (A16) through (A 25) in Appendix A. The coefficients A_1, A_2 are defined as:

$$A_1 = \left(\frac{c_{13}\lambda_2+c_{23}}{\lambda_2+1}\right)(r_2^{\lambda_2+1}-r_1^{\lambda_2+1}) \text{ for } c_{11}\neq c_{22},$$
$$= (c_{23}-c_{13})\ln(r_2/r_1) \quad \text{for } c_{11}=c_{22},$$
$$\cdots\cdots (29a)$$

$$A_2 = \frac{(r_2^2-r_1^2)}{2}\left(c_{33}+\frac{c_{23}^2-c_{13}^2}{c_{11}-c_{22}}\right) \quad \text{for } c_{11}\neq c_{22},$$
$$= \frac{(r_2^2-r_1^2)}{8c_{11}}[4c_{33}c_{11}-(c_{23}-c_{13})^2]+\frac{c_{23}^2-c_{13}^2}{4c_{11}}$$
$$r_2^2\ln(r_2/r_1) \text{ for } c_{11}=c_{22}, \quad \cdots\cdots (29b)$$

Therefore the constants f_j, G_{ij} and hence the displacement U can be found by solving (25) and (28). After obtaining the displacement field, the stresses can be found by substituting in (6) and (3). The specific results are presented in the next section.

3. Discussion of Results

First, a significant observation is that due to the slow rate of moisture diffusion process, many terms, i.e. roots α_n of the characteristic e-

quation (2e), are needed, which makes the Hankel asymptotic regime very important. In the results presented in this section, fifteen terms were used.

As an illustrative example, a T300/5208 Gr/Ep circular cylinder of inner radius r_1 = 20mm and radii ratio r_2/r_1 = 1.50 was considered. The fibers are oriented along the circumferential direction. The typical values of moduli in GN/m^2 and Poisson's ratios are:

$$E_1 = 9.9, E_2 = 140, E_3 = 9.1,$$
$$G_{23} = 4.3, G_{12} = 4.7, G_{31} = 5.9,$$
$$\nu_{12} = 0.020, \nu_{23} = 0.30, \nu_{31} = 0.49,$$

where 1 is the radial(r), 2 is the circumferential(θ) and 3 is the axial(z) direction.

The typical values of hygroscopic expansion coefficients (e.g., Hahn[4]) are: $\beta_r = \beta_z = 6.67\times10^{-3}$/wt%, $\beta_\theta = 0$. For this material, the moisture diffusivity in the radial direction is D = 2.145x 10^{-13} m^2/sec. This value was obtained by substituting a temperature of 50℃ to the equation for the temperature-dependent moisture diffusivity in Hahn [4]. To illustrate the results, the nondimensional radial distance $\bar{r} = (r - r_1)/(r_2 - r_1)$, and normalized time $\bar{t} = Dt/(r_2 - r_1)^2$ are used. The initial concentration (at $t = 0$) is taken C_0 = 0.1, whereas the concentrations at the ends for $t > 0$ are: C_1 = 0.5 and C_2 = 1.5.

Fig. 3.1 shows the spatial distribution of the concentration. Two time values, $\bar{t}$ = 0.002 (corresponding to about 10 days) and $\bar{t}$ =0.01 (corresponding to about 50 days) are used.

The major stresses are the hoop, $\sigma_{\theta\theta}$ and the axial one σ_{zz} , and these are shown in Figs. 3.2, 3.3. The boundary-layer effect is more clearly shown in the axial stress. Notice that these plots illustrate the cases with no mechanical load present, i.e. these stresses are induced purely from the hygroscopic effects. Although a normalization of the stresses would be generally desirable in presenting the results, it is

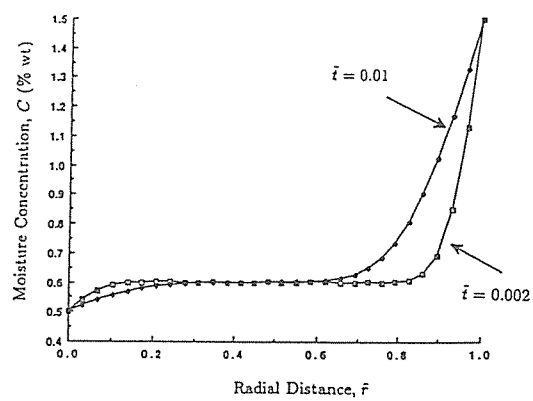

Fig. 3.1. Radial Distribution of the Concentration $C(r,t)$ at Different Times.
The Nondimensional Time is Defined by $\bar{t} = Dt/(r_2 - r_1)^2$.
The Nondimensional Radial Distance is Defined by $\bar{r} = (r - r_1)/(r_2 - r_1)$.

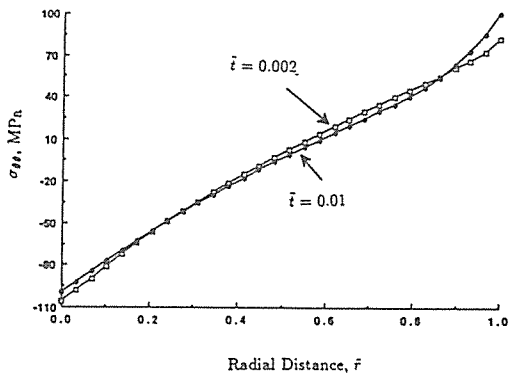

Fig. 3.2. Distribution of the Hoop Stress $\sigma_{\theta\theta}$ (NO Mechanical Loading).

my opinion that for this particular hygroelastic problem, absolute values give a more clear description of the resulting effects.

It should also be mentioned that longer time scales are used because the equlibrium process of moisture absorption or desorption takes much longer than that of temperature.

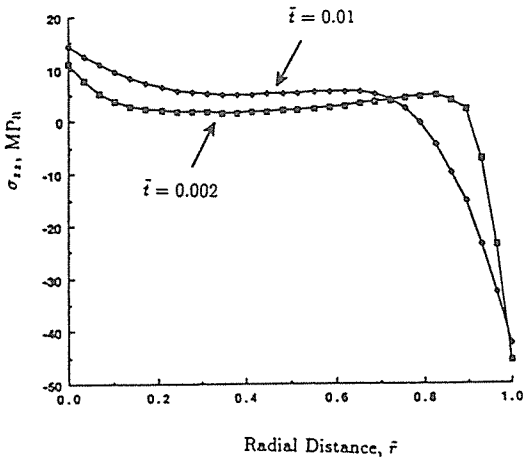

Fig. 3.3. Distribution of the Axial Stress σ_{zz} (No Mechanical Loading).

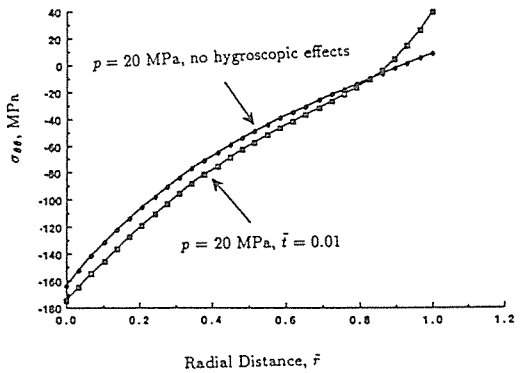

Fig. 3.4. Distribution of the Hoop Stress $\sigma_{\theta\theta}$, Illustrating the Coupling of Mechanical Loading (External Pressure) and Hygroscopic Effects.

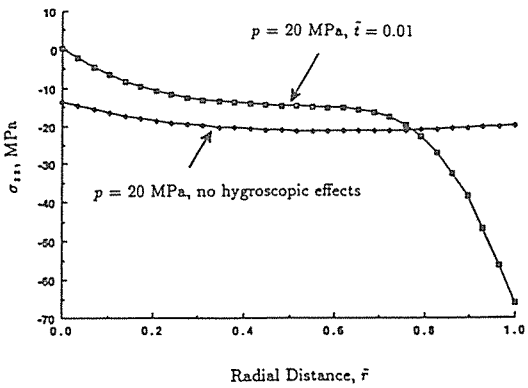

Fig. 3.5. Distribution of the Axial Stress σ_{zz}, Illustrating the Coupling of Mechanical Loading (External Pressure) and Hygroscopic Effects.

The coupling of mechanical loading and hygroscopic effects is illustrated in Figs. 3.4, 3.5, which show the hoop stress, $\sigma_{\theta\theta}$, and the axial one, σ_{zz}, for (a) applied external pressure only and (b) applied external pressure with consideration of the hygroscopic effects at time $\bar{t}$ = 0.01. The stress distribution for hydrostatic pressure only is taken from Lekhnitskii[12]. It is seen that the hygroscopic effects result in an increase in the absolute value of the hoop stress at both the inner and outer boundaries.

Again the hygroscopic boundary-layer is more clearly seen in the axial stress σ_{zz}, which shows a large increase near the outer surface. In this example, a value of the external pressure $p = 20$ MPa was taken. Other values of the hydrostatic pressure would affect mainly the mean value and not the existence of the boundary layer stress.

More specifically, Fig. 3.6 shows the effect of coupled applied pressure p, and hygroscopic fields, on the axial stress, for p = 0 (only hygroscopic effects), p = 5 and p = 20 MPa at time $\bar{t}$ = 0.002.

Notice also that for the example considered, the reinforcement is along the periphery, thus the axial direction is a direction of weakness. Therefore, the boundary-layer effect on the axial stress may have more important implications for failure initiation than a similar one on the hoop component. Applications of thick composite shells in marine environments

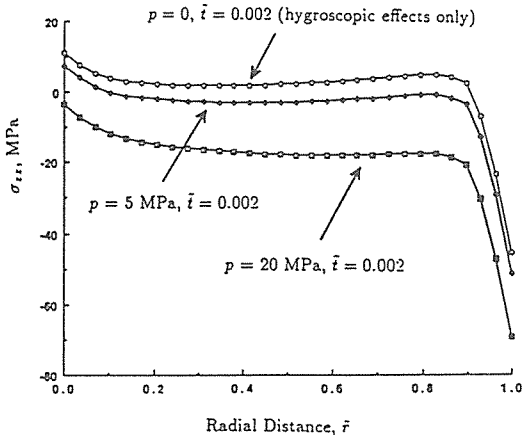

Fig. 3.6. Distribution of the Hoop Stress σ_{zz}, Illustrating the Effect of Variable Mechanical Loading (External Pressure), Coupled with the Hygroscopic Effects.

may actually involve a larger size than the one considered in these examples.

For an insight into these size effects, the results for the transient stress profiles were derived for a shell made out of the same material with the same fiber orientation, and of inner radius r_1 = 4m and radii ratio r_2/r_1 = 1.25. A time value of 50 days with no mechanical loading and the same initial and boundary moisture concentrations were used.

It turns out that the same boundary-layer effect on the axial stress σ_{zz} appears (as in the present, smaller size example, Fig. 3.3, $\bar{t}$ = 0.01), with a similar range of negative values; however, the boundary layer was confined to a smaller $\bar{r}$ range near the outer surface. A much smaller effect exists for the hoop stress $\sigma_{\theta\theta}$, with smaller positive and less negative values than in the small size example, Fig. 3.2.

Equations (B4) through (B10) in Appendix B represent the resultant stresses and moments induced by moisture absorption for an orthotropic body. Since they are integrated with respect to the radial distance, it is noteworthy to observe that the classical shell theory cannot capture the boundary-layer stresses characteristic of which the dependence of the radial coordinate is for this problem.

Reference

1. C.E. Browning, G.E. Husman, and J.M. Whitney, "Moisture Effects in Epoxy Matrix Composites," Composite Materials: Testing and Design (Fourth Conference), ASTM STP 617, American Society for Testing and Materials, 1977, pp.481-496.

2. J.M. Whitney and G.E. Husman, "Use of the Flexure Test for Determining Environmental Behavior of Fibrous Composites," Experimental Mechanics, Vol. 8, No. 5, May 1978, pp.185-190.

3. R. DeIasi and J.b. Whiteside, "Effect of Moisture on Epoxy Resins and Composites," Advanced Composite Materials-Environmental Effects, ASTM STP 658, American Society for Testing and Materials, 1978, pp.2-20.

4. H.T. Hahn, "Residual Stresses in Polymer Matrix Composite Laminates," J. Composite Materials, Vol. 10, October 1976, pp.266-278.

5. H.T. Hahn and R.Y. Kim, "Swelling of Composite Laminates," Advanced Composite Materials-Environmental Effects, ASTM STP 658, American Society for Testing and Materials, 1978, pp.98-120.

6. H.T. Hahn and K.S. Kim, "Hygroscopic Effects in Aramid Fiber/Epoxy Composite," Journal of Engineering Materials and Technology, Vol. 110, April 1988, pp.153-157.

7. F.W. Crossman, R.E. Mauri and W.J. Warren, "Moisture-Altered Viscoelastic Response of Graphite/Epoxy Composites," Advanced Composite Materials-Environmental Effects, ASTM STP 658, American Society for Testing and Materials, 1978, pp.205-220.

8. B.D. Harper, "The Effects of Moisture Induced Swelling upon the Shapes of Anti-Symmetric Cross-Ply Laminates," Journal of Com-

posite Materials, Vol. 21, January 1987, pp.36-48.

9. R.B. Pipes, J.R. Vinson and T.W. Chou, " On the Hygrothermal Response of Laminated Composite Systems," Journal of Composite Materials, Vol. 10, April 1976, pp.129-148.

10. G.A. Kardomateas, "Transient Thermal Stresses in Cylindrically Orthotropic Composite Tubes," Journal of Applied Mechanics, Vol. 56, June 1989, pp.411-417, also Errata, Ibid, Vol. 58, 1991, p.909.

11. G.A. Kardomateas, "The Initial Phase of Transient Thermal Stresses due to General Boundary Thermal Loads in Orthotropic Hollow Cylinders," Journal of Applied Mechanics, Vol. 57, September 1990, pp.719-724, also Errata, Ibid, Vol. 58, 1991, p.909.

12. S.G. Lekhnitskii, "Theory of Elasticity of an Anisotropic Elastic Body," Mir Publishers, 1981.

13. C.B. Chung and G.A. Kardomateas, " Moisture Induced Transient Stresses in Orthotropic, Thick Shells under Pressure," SECTAM XVI Conference, Nashiville Tennessee, April 1991, pp.II.15.1-II.15.8.

14. C.B. Chung, "Hygroscopic Stresses in Orthotropic, Thick Shells under Pressure," submitted, J. of the Korean Society for Composite Materials, Republic of Korea.

15. L.E. Doxee, Jr. and G.S. Springer, "Hygrothermal Stresses and Strains in Axisymmetric Composite Shells," Computers and Structures, Vol. 32, No. 2, 1989, pp.395-407.

16. L.E. Doxee, Jr., "A Higher-Order Theory of Hygrothermal Behavior of Laminated Composite Shells," Int. J. Solids Structures, Vol. 25, No. 4, 1989, pp.339-355.

17. G.L. Farley and C.T. Herakovich, "Influence of Two-Dimensional Hygrothermal Gradients on Interlaminar Stresses Near Free Edges," Advanced Composite Materials-Environmental Effects, ASTM STP 658, American Society for Testing and Materials, 1978, pp.143-159.

18. S.S. Wang and I. Choi, "Boundary-Layer Hygroscopic Stresses in Angle-Ply Composite Laminates," AIAA Journal, Vol. 20, No. 11, November 1982, pp.1592-1598.

19. J. Crank, "The Mathematics of Diffusion," 2nd ed., published by Clarendon Press, 1975.

20. Wylie C. Ray, "Advanced Engineering Mathematics," 4th ed., published by McGraw-Hill Book Company, New York, 1975.

21. Abramowitz M. and Stegun I.A., "Handbook of Mathematical Functions with Formulas, Graphs, and Mathematical Tables," National Beureau of Standards Applied Mathematics Series No. 55, 9th Printing, Washington, D. C., 1970.

22. D.O. Brush and B.O. Almroth, "Buckling of Bars, Plates, and Shells," McGraw-Hill, New York, 1975.

APPENDIX A

Bessel Functions And Supplementary Equations

The Bessel functions are classified as for small arguments and for large arguments. The full expressions for the supplementary equations cited in Section 2 are given.

A-1. Bessel Functions

The Bessel functions of first and second kind of order zero and one have a seriesexpansion of the form (see e.g. Wylie[20])

$$J_0(x)=\sum_{k=0}^{\infty}\frac{(-1)^k x^{2k}}{2^{2k}(k!)^2}\ ;\ J_1(x)=\sum_{k=0}^{\infty}\frac{(-1)^k x^{2k+1}}{2^{2k+1}k!(k+1)!}\ , \qquad \text{(A1)}$$

$$Y_0(x)=\frac{2}{\pi}(\ln\frac{x}{2}+\gamma)J_0(x)-\frac{2}{\pi}\sum_{k=1}^{\infty}\frac{(-1)^k x^{2k}}{2^{2k}(k!)^2}\psi(k)\ , \qquad \text{(A2)}$$

$$Y_1(x)=\frac{2}{\pi}(\ln\frac{x}{2}+\gamma)J_1(x)-\frac{2}{\pi}\frac{1}{x}-\frac{1}{\pi}\sum_{k=0}^{\infty}\frac{(-1)^k x^{2k+1}}{2^{2k+1}(k!)(k+1)!}\left[2\psi(k+1)-\frac{1}{k+1}\right]. \qquad \text{(A3)}$$

In the above expressions γ= 0.577215... is the Euler's constant and $\psi(k)$ is defined as

$$\psi(k)=1+\frac{1}{2}+\cdots+\frac{1}{k}\ . \qquad \text{(A4)}$$

The above series expansions can be used to calculate the Bessel's functions up to a value of the argument of about x = 18. They are rapidly convergent especially for small values of the argument.

Using the series expansion, we obtain the following equation in place of (10b):

$$c_{11}(R_n''(r)+\frac{R_n'(r)}{r})-\frac{c_{22}}{r^2}R_n(r)=\frac{(c_{23}-c_{13})f_n}{r}+\frac{c_n q_2+(2/\pi)(q_1+\gamma q_2)d_n}{r}+$$
$$+\frac{2d_n q_2}{\pi}\frac{\ln(r\alpha_n/2)}{r}+\frac{2d_n}{\pi}\sum_{k=0}^{\infty}\frac{(-1)^{k+1}\alpha_n^{2k+2}[q_2+2q_1(k+1)]}{2^{2k+2}[(k+1)!]^2}r^{2k+1}\ln(r\alpha_n/2)+\sum_{k=0}^{\infty}\frac{(-1)^{k+1}\alpha_n^{2k+2}f_{kn}}{2^{2k+2}[(k+1)!]^2}r^{2k+1}\ , \qquad \text{(A5)}$$

where f_{kn} is defined in (13d).

For *large arguments* we can use the Hankel asymptotic expansions for the Bessel functions (see e. g. Abramowitz and Stegun[21]) to obtain the following expressions

$$J_0(x)=A_0(x)\sin x+B_0(x)\cos x\ ;\ J_1(x)=B_1(x)\sin x-A_1(x)\cos x\ , \qquad \text{(A6)}$$

$$Y_0(x)=B_0(x)\sin x-A_0(x)\cos x\ ;\ Y_1(x)=-A_1(x)\sin x-B_1(x)\cos x\ . \qquad \text{(A7)}$$

The functions $A_0(x)$, $A_1(x)$, $B_0(x)$, $B_1(x)$ are given in terms of

$$\psi_1(k) = 1^2.3^2.5^2\cdots(4k-1)^2\,,\ k=1,\infty\,;\quad \psi_1(0)=1\,, \qquad \text{(A8)}$$

as follows

$$(\pi x)^{1/2}A_0(x) = \sum_{k=0}^{\infty} \frac{(-1)^k\,\psi_1(k)}{(2k)!(8x)^{2k}}\left[1-\frac{16kx}{(4k-1)^2}\right], \qquad \text{(A9)}$$

$$(\pi x)^{1/2}A_1(x) = \sum_{k=0}^{\infty} \frac{(-1)^{k+1}\psi_1(k)(4k+1)}{(2k)!(8x)^{2k}(4k-1)}\left[1-\frac{16kx}{(4k-3)(4k+1)}\right], \qquad \text{(A10)}$$

$$(\pi x)^{1/2}B_0(x) = \sum_{k=0}^{\infty} \frac{(-1)^k\,\psi_1(k)}{(2k)!(8x)^{2k}}\left[1+\frac{16kx}{(4k-1)^2}\right], \qquad \text{(A11)}$$

$$(\pi x)^{1/2}B_1(x) = \sum_{k=0}^{\infty} \frac{(-1)^{k+1}\psi_1(k)(4k+1)}{(2k)!(8x)^{2k}(4k-1)}\left[1+\frac{16kx}{(4k-3)(4k+1)}\right]. \qquad \text{(A12)}$$

In this way, the above series of the Hankel asymptotic expansion can be used to calculate the Bessel functions for values of the argument $x \geq 18$. The series converges rapidly and the number of terms required in the summation over k is at most 13 at x = 18.0, being smaller for larger values of the argument.

A-2. Supplementary Equations

In the event that for a certain k, $c_{11}(2k+3)^2 = c_{22}$, the term in the sum in (13b) and (15b) for this k is

$$B_{1nk}\,r^{2k+3}\ln^2(r\,\alpha_n/2) + B_{2nk}\,r^{2k+3}\ln(r\,\alpha_n/2)\,, \qquad \text{(A13)}$$

where now

$$B_{1nk} = \frac{2d_n(-1)^{k+1}\alpha_n^{2k+2}\,[q_2+2q_1(k+1)]}{\pi\,2^{2k+2}[(k+1)!]^2\,4c_{11}(2k+3)}\,, \qquad \text{(A14)}$$

$$B_{2nk} = \frac{(-1)^{k+1}\alpha_n^{2k+2}}{2^{2k+2}\,[(k+1)!]^2 2c_{11}(2k+3)}\left\{f_{kn}-\frac{2d_n\,[q_2+2q_1(k+1)]}{2\pi(2k+3)}\right\}. \qquad \text{(A15)}$$

For $c_{11} \neq c_{22}$, the expression for I_0 in (28a), is:

$$I_0 = \frac{q_2(b_1r_2^2-b_2r_1^2)}{2(c_{11}-c_{22})}\ln(r_2/r_1) + \left[\frac{(2q_1-q_2)}{4(c_{11}-c_{22})} - \frac{q_2c_{11}}{(c_{11}-c_{22})^2}\right](b_1-b_2)(r_2^2-r_1^2), \qquad \text{(A16)}$$

and the expressions for I_n, $n = 1,\cdots\infty$, in (28b), for the small arguments domain, are

$$I_n = \sum_{i=1,2}(-1)^i \frac{r_i^2}{2}\left[B_{0n} - \frac{d_n q_2}{\pi(c_{11}-c_{22})}\right] + (-1)^i \frac{d_n q_2}{\pi(c_{11}-c_{22})} r_i^2 \ln(r_i \alpha_n/2) + S_n \,, \quad \text{(A17)}$$

$$S_n = \sum_{i=1}^{2}\sum_{k=0}^{\infty}(-1)^i B_{1nk} \frac{r_i^{2k+4}}{2k+4} \ln(r_i \alpha_n/2) + (-1)^i [B_{2nk} - \frac{B_{1nk}}{2k+4}] \frac{r_i^{2k+4}}{2k+4} \,. \quad \text{(A18)}$$

For $c_{11} = c_{22}$, the expression for I_0 is

$$8 I_0 c_{11} = q_2(b_1 r_2^2 + b_2 r_1^2)\ln^2(r_2/r_1) + (q_2 - q_1)(b_1 - b_2)(r_2^2 - r_1^2) + \\ + [(2q_1 - q_2)(b_1 - b_2) r_2^2 + q_2(b_2 r_1^2 - b_1 r_2^2)] \ln(r_2/r_1) \,, \quad \text{(A19)}$$

and the expressions for I_n, n=1,$\cdots\infty$, again in the small arguments domain, are

$$I_n = \sum_{i=1,2}(-1)^i \frac{d_n q_2}{\pi 4 c_{11}} r_i^2 \ln^2(r_i \alpha_n/2) + (-1)^i (\frac{B_{0n}}{2} - \frac{d_n q_2}{\pi 4 c_{11}}) r_i^2 \ln(r_i \alpha_n/2) + (-1)^{i+1} (\frac{B_{0n}}{2} - \frac{d_n q_2}{\pi 4 c_{11}}) \frac{r_i^2}{2} + S_n \,. \quad \text{(A20)}$$

For large arguments, with $\rho_i = r_i \alpha_n$,

$$\alpha_n I_n = \sum_{i=1,2}(-1)^i \sum_{k=0}^{\infty}(p_{k,1}^n + \frac{s_{k,2}^n}{2k+1/2}) I_{c,k}(\rho_i) + (s_{k,1}^n - \frac{p_{k,2}^n}{2k+1/2}) I_{s,k}(\rho_i) - \frac{p_{k,2}^n}{2k+1/2} \rho_i^{-2k-1/2} \cos\rho_i - \\ \frac{s_{k,2}^n}{2k+1/2} \rho_i^{-2k-1/2} \sin\rho_i \,, \quad \text{(A21)}$$

where $I_{c,k}(\rho)$ and $I_{s,k}(\rho)$ are defined by the recursive formulas

$$(2k-1/2)(2k-3/2) I_{c,k} = -(2k-3/2)\rho^{-2k+1/2}\cos\rho + \rho^{-2k+3/2}\sin\rho - I_{c,k-1} \,, \quad \text{(A22)}$$

$$(2k-1/2)(2k-3/2) I_{s,k} = -(2k-3/2)\rho^{-2k+1/2}\sin\rho - \rho^{-2k+3/2}\cos\rho - I_{s,k-1} \,. \quad \text{(A23)}$$

The process starts from k=0, and initially,

$$I_{c,0}(\rho) = \int \rho^{-1/2}\cos\rho d\rho \,; \quad I_{s,0}(\rho) = \int \rho^{-1/2}\sin\rho d\rho \,. \quad \text{(A24)}$$

Notice that the integral of the homogeneous solution (22a) (due to continuity requirements at the transition point of the two partial solutions) should be added to I_n, *i.e.*, for $c_{11} \neq c_{22}$, the following term should be added:

$$\sum_{i=1,2}(-1)^i (h_1 \frac{\rho_i^{\lambda_1+1}}{\lambda_1+1} + h_2 \frac{\rho_i^{\lambda_2+1}}{\lambda_2+1}) \,. \quad \text{(A25)}$$

For $c_{11} = c_{22}$, the term multiplying h_2 in the previous relation (A25) is $\ln\rho_i$.

APPENDIX B

Shell Theory Including Hygroscopic Stresses

Equilibrium equations for a nonshallow circular cylinder can be derived by using the principle of the stationary value of total potential energy (see also Brush and Almroth[22]).

$$RN_{z,z}+N_{z\theta,\theta}=0\,, \quad \text{(B1)}$$

$$RN_{z\theta,z}+N_{\theta,\theta}-N_{\theta}\Phi_{\theta}-N_{z\theta}\Phi_{z}+\frac{1}{R}M_{\theta,\theta}+M_{z\theta,z}-p\,(v-u_{,\theta})=0\,, \quad \text{(B2)}$$

$$RM_{z,zz}+2M_{z\theta,\theta z}+\frac{1}{R}M_{\theta,\theta\theta}-N_{\theta}-[(N_{\theta}\Phi_{\theta})_{,\theta}+(N_{z\theta}\Phi_{z})_{,\theta}+R(N_{z\theta}\Phi_{\theta})_{,z}+R(N_{z}\Phi_{z})_{,z}]-p\,(R+u+v_{,\theta})=0\,, \quad \text{(B3)}$$

where $R\Phi_{\theta}=(v-u_{,\theta})$ and $\Phi_{z}=-u_{,z}$. The resultant forces and moments including hygroscopic stresses are differed by two terms. The one is induced from the total strains and the other from hygroscopic field.

$$N_{ij}=N_{ij}^{t}-N_{ij}^{m}\,, \quad \text{(B4)}$$

$$M_{ij}=M_{ij}^{t}-M_{ij}^{m}, \quad i,j=\theta,\,z \quad \text{(B5)}$$

where N_{ij}^{t} and M_{ij}^{t} are due to the total strains, and N_{ij}^{m} and M_{ij}^{m} due to the strains induced by moisture absorption. For an orthotropic body in the axisymmetric case like our problem,

$$N_{\theta}^{m}=\int_{r_1}^{r_2}(q_1-q_2)\,\Delta C\,(r,\theta,z,t)\,dr\,, \quad \text{(B6)}$$

$$N_{z}^{m}=\int_{r_1}^{r_2}q_3\,\Delta C\,(r,\theta,z,t)\,dr\,, \quad \text{(B7)}$$

$$N_{\theta z}^{m}=M_{\theta z}^{m}=0\,, \quad \text{(B8)}$$

$$M_{\theta}^{m}=\int_{r_1}^{r_2}(q_1-q_2)\,\Delta C\,(r,\theta,z,t)\,(r-R)\,dr\,, \quad \text{(B9)}$$

$$M_{z}^{m}=\int_{r_1}^{r_2}q_3\,\Delta C\,(r,\theta,z,t)\,(r-R)\,dr\,, \quad \text{(B10)}$$

where $C(r,\theta,z,t)$ is the concentration of moisture and q_1, q_2, q_3 and R are the same as defined previously.